

Design of a spiral inflector at iThemba LABS for injection of the beam into a cyclotron

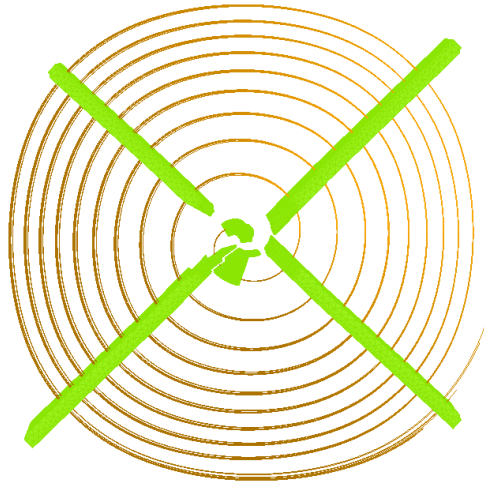
Hugo Barnard
hbarnard@tlabs.ac.za
iThemba LABS

December 2022
Cyclotron2022 – Beijing

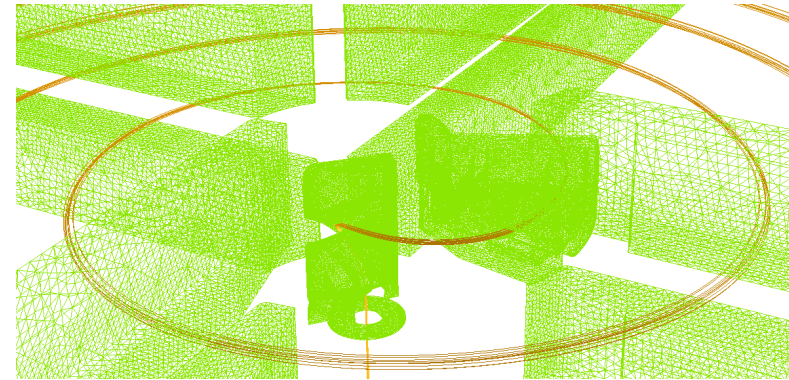
Overview of Talk

- Background on spiral inflectors
- Previous work at iThemba optimising a spiral inflector
- Permanent magnet spiral inflectors
- Optimising: Cyclotron acceptance, injection beam line
- New electrostatic simulation
- Results: Electric vs Magnetic

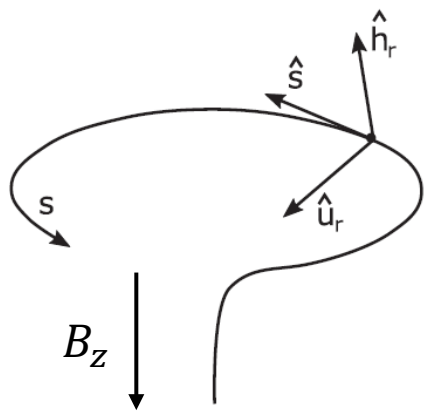
Background – Spiral Inflector



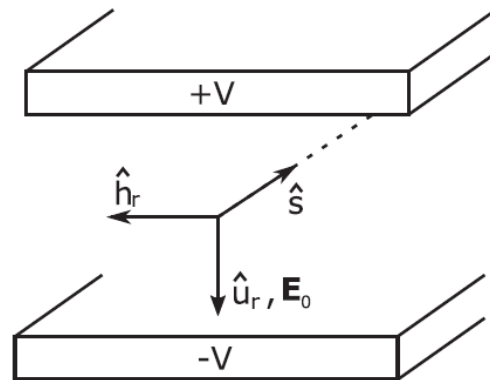
Inflector in central region



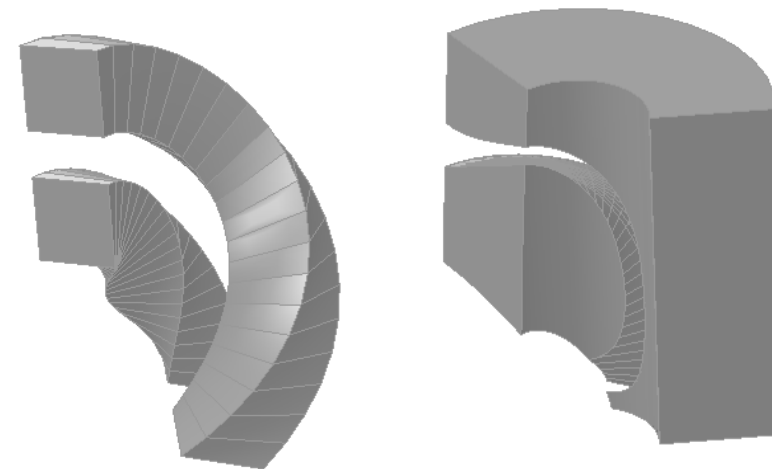
Axial injection



Magnetic field constant
(except in axial hole)



E field between electrodes

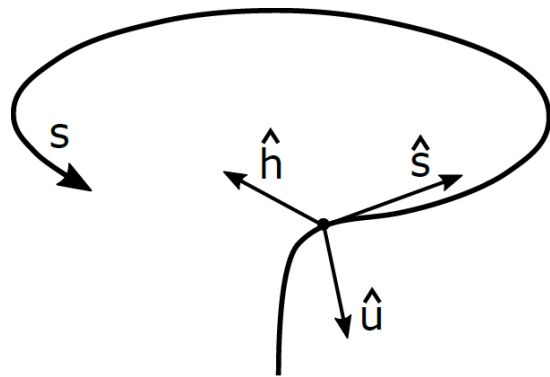


Electrodes

Background – Central path

Low energy non-relativistic

$$\ddot{\mathbf{x}} = \frac{q}{m} \mathbf{E} + \frac{q}{m} \dot{\mathbf{x}} \times \mathbf{B}$$



Coordinate system (u, h, s) :

\hat{s} - direction of motion

\hat{h} - horizontal

\hat{u} - given by: $\hat{u} = \hat{h} \times \hat{s}$

Criteria for central path:

- $\phi = 0$, so $E_s = 0$
- Analytical solution

“Spiral inflector” has:

1. Constant E_u . This is equivalent to a linear vertical field:

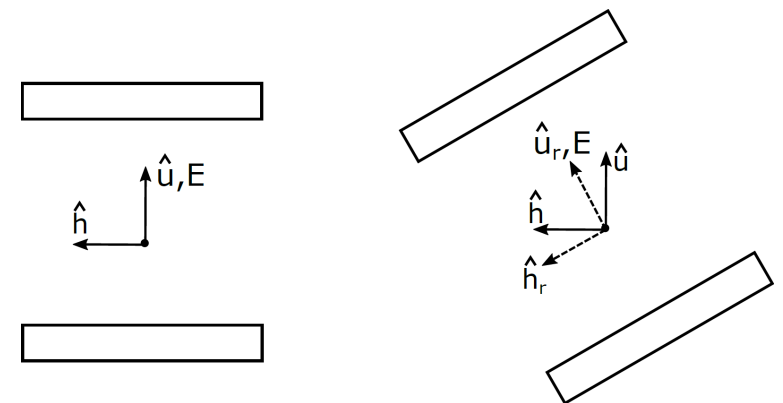
$$E_z = -k z$$

2. E_h is selected so it is proportional to the magnetic force. This creates an “effective” magnetic field

For a given magnetic bending radius R_m , the free parameters are:

A – height

k' – tilt parameter:



Properties of Inflector C for the SPC2:

R_m	4.9 cm
A	6.0 cm
k'	0.38

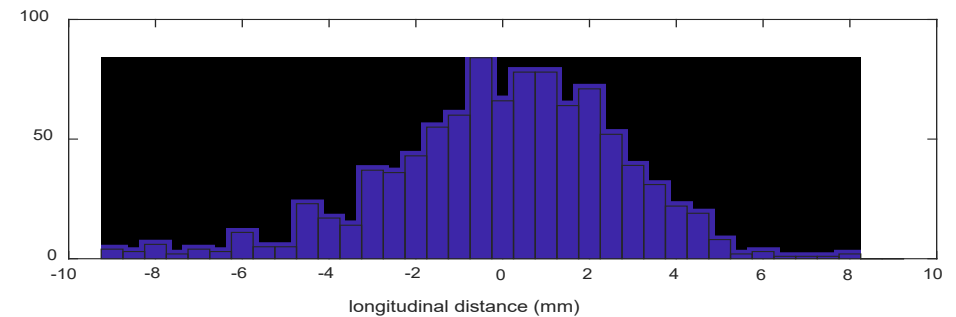
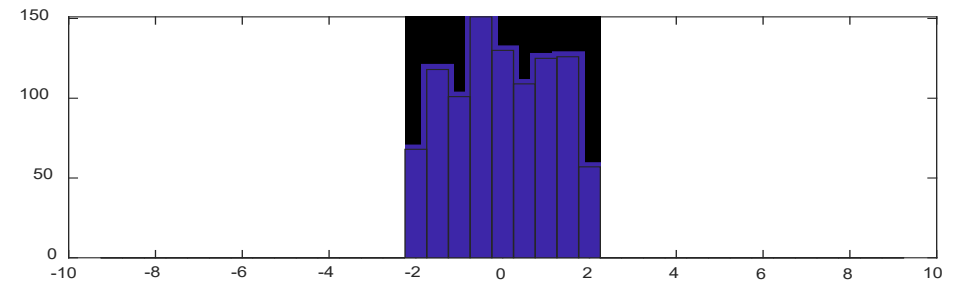
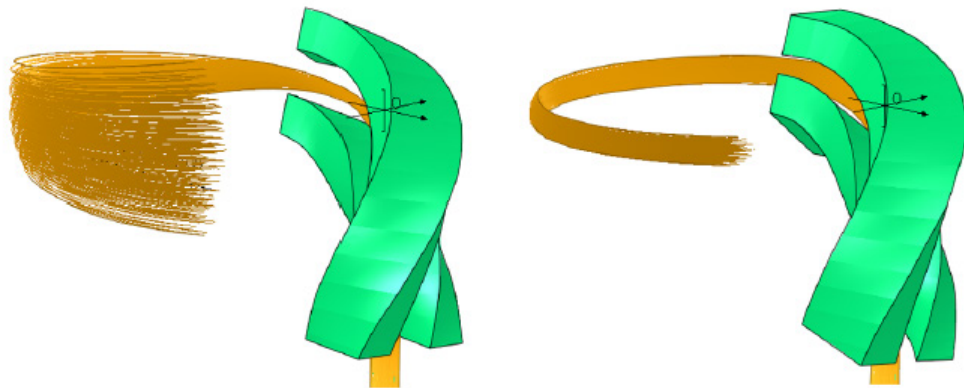
Background - Problems

- Emittance blow-up from coupling (6D unchanged, projected 2D can grow)
- Significant vertical spread
Central region – no magnetic focusing
- Longitudinal de-bunching

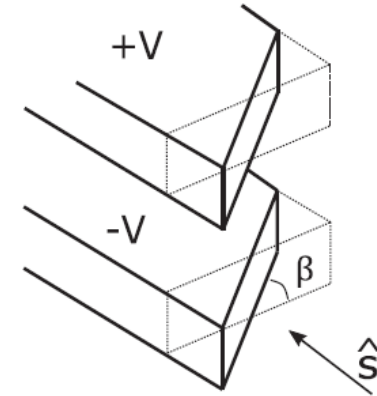
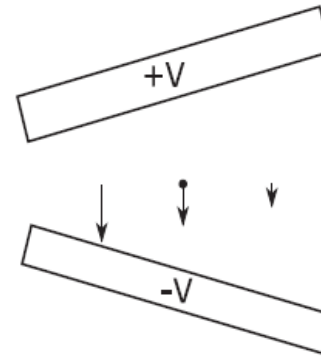
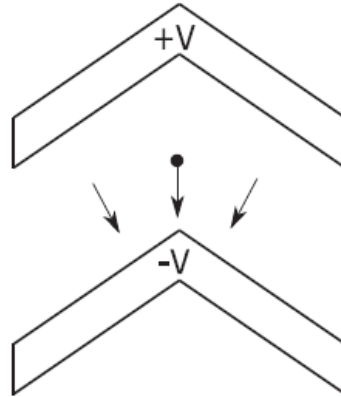
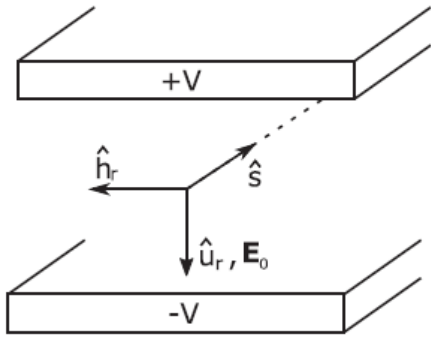
TABLE III. Transfer matrix R of C1 ($|R| = 1.00$).

-1.3078	-0.0216	-2.1882	-0.2905	0	-0.2462
-10.951	-0.2732	-21.255	-3.2250	0	-1.9985
0.8273	0.0470	-0.3371	-0.0648	0	-0.0166
-2.3343	0.9307	-3.7095	-1.0723	0	-1.5982
1.4403	0.0834	0.3830	0.1273	1	0.1793
-0.0027	-0.0015	0.0276	0.0031	0	1.0016

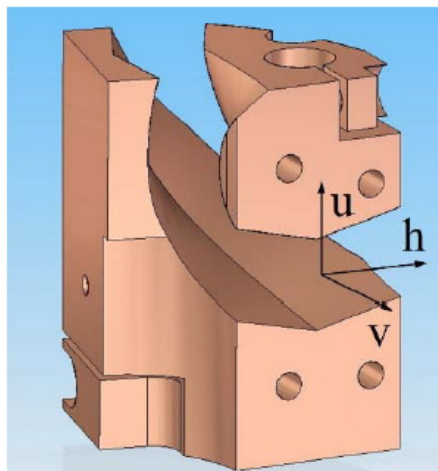
Source [1]



Previous Work – Transverse Gradients

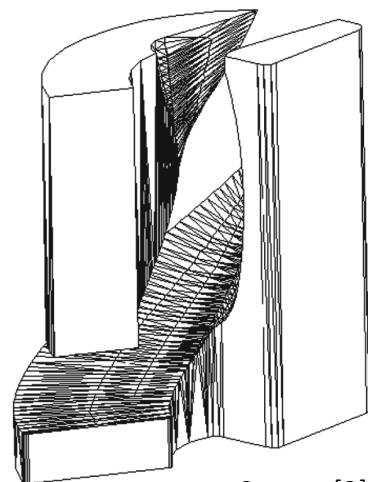


Dubna (1)



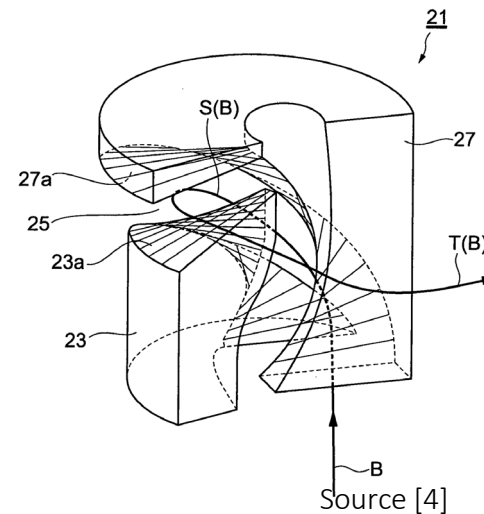
Source [2]

Dubna (2)



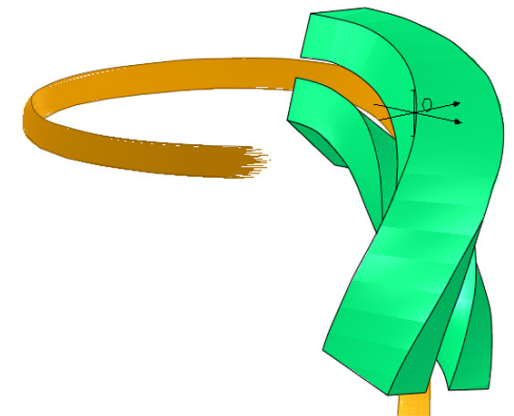
Source [3]

Sumitomo



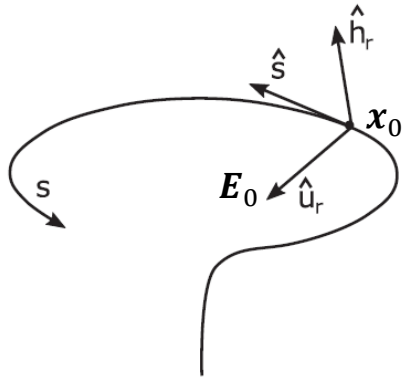
Source [4]

iThemba (C2)



Previous Work – Electric potential

Rotated (u_r, h_r, s) coordinate frame aligned with main electric field: $\mathbf{E}_0 = E_0 \hat{u}_r$



$$\mathbf{x}(u_r, h_r, s) = \mathbf{x}_0(s) + u_r \hat{u}_r(s) + h_r \hat{h}_r(s)$$

Rotation of coordinate frame - κ

$$\hat{u}'_r = \kappa_s \hat{h}_r - \kappa_h \hat{s}$$

$$\hat{h}'_r = \kappa_u \hat{s} - \kappa_s \hat{u}_r$$

$$\hat{s}'_r = \kappa_h \hat{u}_r - \kappa_u \hat{h}_r$$

Coordinates form a non-orthogonal system, with base and dual base vectors:

$$\mathbf{b}_1 = \frac{\partial \mathbf{x}}{\partial u_r} = \hat{u}_r$$

$$\mathbf{b}_2 = \frac{\partial \mathbf{x}}{\partial h_r} = \hat{h}_r$$

$$\mathbf{b}_3 = \frac{\partial \mathbf{x}}{\partial s} = \hat{s}_r (1 - u_r \kappa_h + h_r \kappa_u) + \kappa_s (u_r \hat{h}_r - h_r \hat{u}_r)$$

$$\mathbf{b}^1 = \hat{u}_r + \frac{h_r \kappa_s}{1 - u_r \kappa_h + h_r \kappa_u} \hat{s}$$

$$\mathbf{b}^2 = \hat{h}_r - \frac{u_r \kappa_s}{1 - u_r \kappa_h + h_r \kappa_u} \hat{s}$$

$$\mathbf{b}^3 = \frac{1}{1 - u_r \kappa_h + h_r \kappa_u} \hat{s}$$

Laplace:

$$\nabla^2 \phi = \frac{1}{\sqrt{g}} \sum_i \frac{\partial}{\partial u^i} \left(\sqrt{g} \sum_j \frac{\partial \phi}{\partial u^j} g^{ij} \right) = 0$$

$g_{ij} = \mathbf{b}_i \cdot \mathbf{b}_j$ is the metric matrix

$$g = \det g_{ij}$$

Expand ϕ to second order in terms of u_r, h_r :

$$\frac{\partial^2 \phi}{\partial u_r^2} + \frac{\partial^2 \phi}{\partial h_r^2} + \hat{s}' \cdot \mathbf{E}_0 = 0$$

This gives \mathbf{E} to first order, i.e. linear optics

Previous Work – Quadrupole parameters

At each point s , the solution is:

$$\phi = -u_r E_0 - Q_1 E_0 \frac{u_r^2 - h_r^2}{2} - Q_2 E_0 h_r u_r - \frac{u_r^2}{2} \hat{s}' \cdot \mathbf{E}_0$$

Quadrupole terms $Q_1(s)$ and $Q_2(s)$ are functions that the inflector designer can select. $Q_1 = Q_2 = 0$ is a traditional inflector.

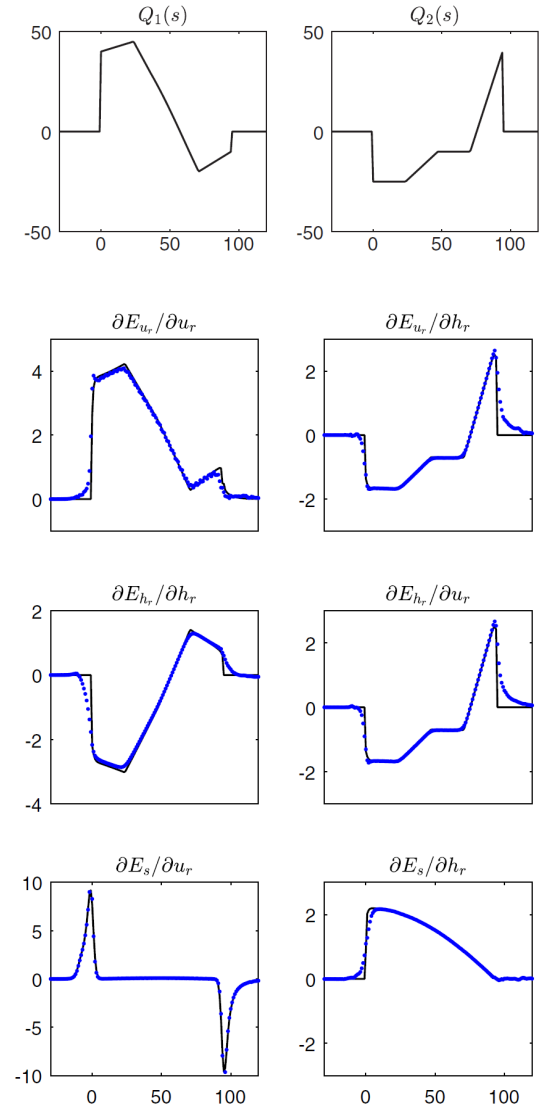
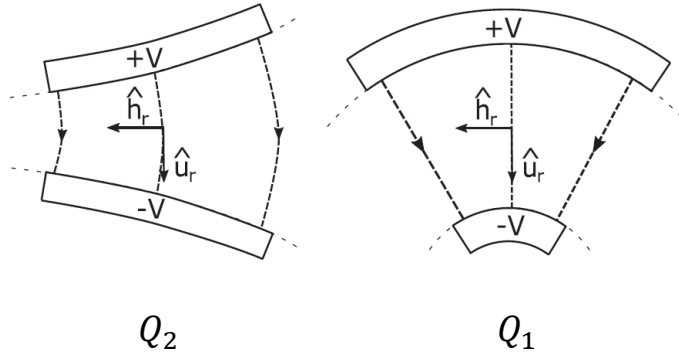
Electric fields:

$$\mathbf{E} = -\nabla\phi = -\sum_i \frac{\partial\phi}{\partial u^i} \mathbf{b}^i$$

$$E_{u_r} = E_0 + u_r(Q_1 E_0 + \hat{s}' \cdot \mathbf{E}_0) + h_r Q_2 E_0$$

$$E_{h_r} = u_r Q_2 E_0 - h_r Q_1 E_0$$

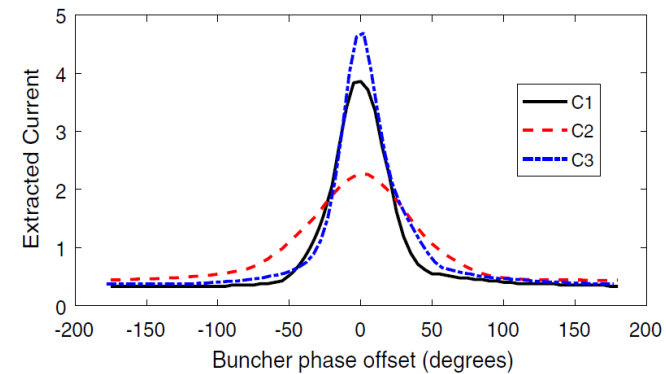
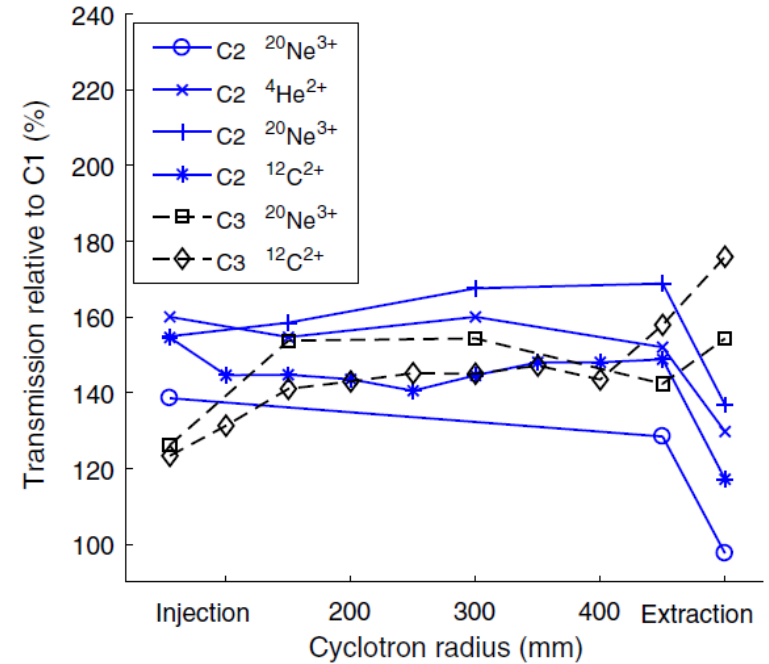
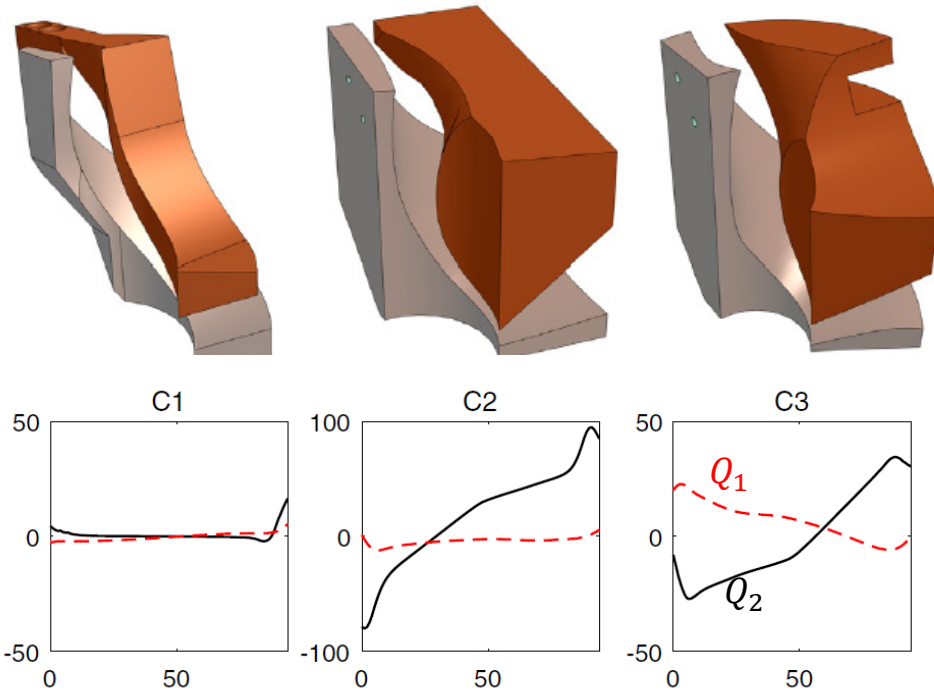
$$E_s = u_r E'_0 - h_r \kappa_s E_0$$



Numerical verification:

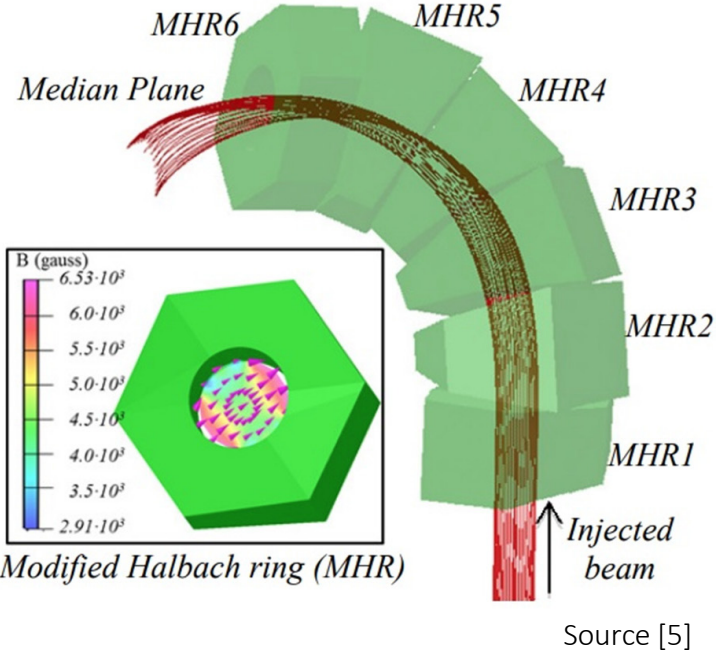
- electrodes lie on equipotential surfaces
- TOSCA and theoretical field gradients agree

Previous Work – Experimental Results



	C1	C2	C3
Vertical emittance	145	105	120
Vertical half width (mm)	8.9	2.9	7.0
Horizontal emittance	145	130	120
Horizontal half width (mm)	3.0	1.5	2.0
Longitudinal half width (mm)	5.5	12.9	3.1
rf phase spread (degrees)	± 39	± 90	± 22

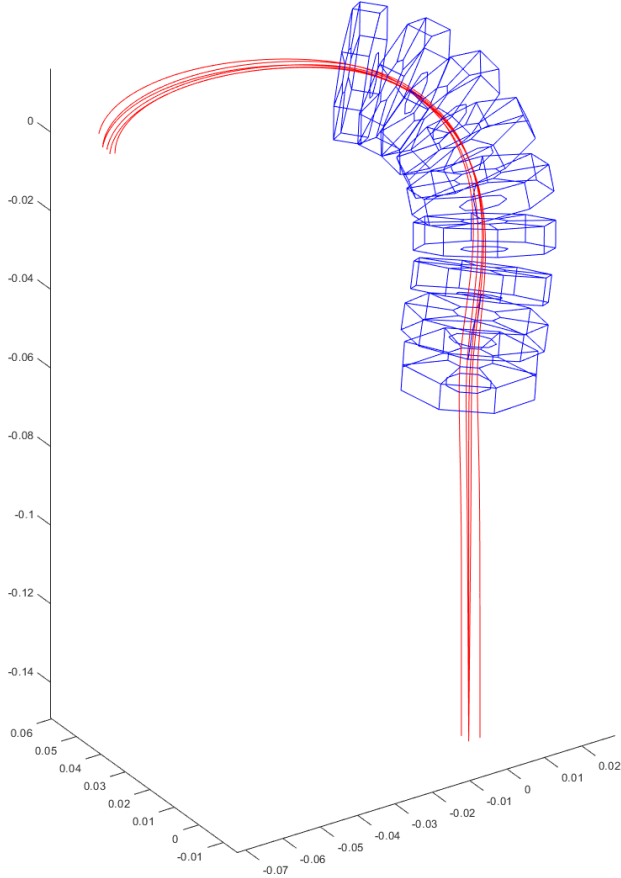
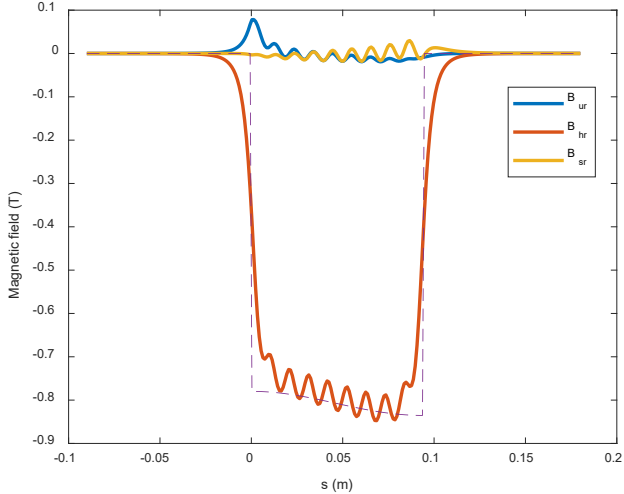
Permanent Magnet Spiral Inflectors



$$F_M = F_E$$

$$E = E_0 \hat{u}_r$$

$$B = -\frac{E_0}{v} \hat{h}_r$$



REVIEW OF HIGH POWER CYCLOTRONS AND THEIR APPLICATIONS

L. Calabretta, D. Rifuggiato, Istituto Nazionale di Fisica Nucleare- LNS, Catania, Italy
 M. Maggiore, Istituto Nazionale di Fisica Nucleare- LNL, Legnaro, Italy

Modified Halbach rings (1)

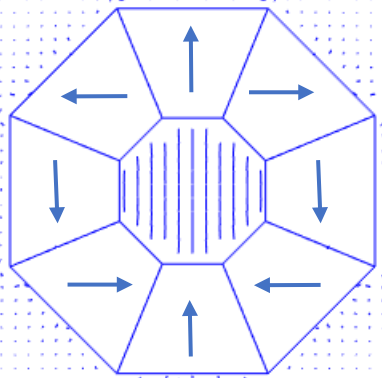
Inflector field: potential similar to electric case

$$B = -\nabla\psi$$

$$\nabla^2\psi = 0$$

$$\psi = h_r B_0 - Q_1 B_0 \frac{u_r^2 - h_r^2}{2} - Q_2 B_0 u_r h_r - \frac{u_r^2}{2} \hat{s}' \cdot \mathbf{B}_0$$

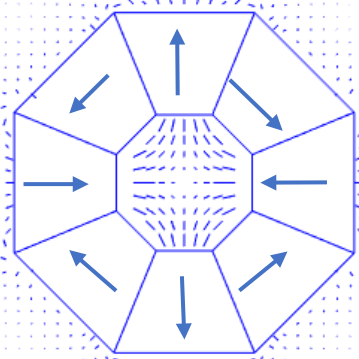
B_0



$$M_r = M_0 \sin \theta$$

$$M_\theta = -M_0 \cos \theta$$

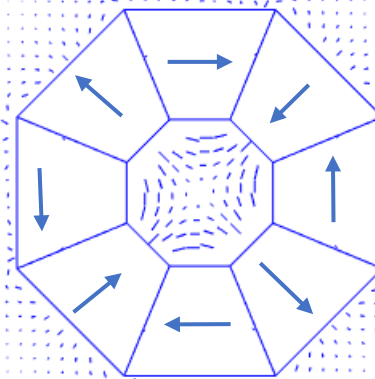
Q_1 type



$$M_r = -M_0 \cos 2\theta$$

$$M_\theta = -M_0 \sin 2\theta$$

Q_2 type



$$M_r = -M_0 \sin 2\theta$$

$$M_\theta = M_0 \cos 2\theta$$

Q_1, Q_2 (field gradients) depend on ring size, spacing etc, so rather work with K_1, K_2 :

$$M_r = M_0 (\sin \theta - K_1 \cos 2\theta - K_2 \sin 2\theta)$$

$$M_\theta = M_0 (-\cos \theta - K_1 \sin 2\theta + K_2 \cos 2\theta)$$

Optimisation space: $K_1(n), K_2(n)$
where $n = 1, \dots$, number of rings

Modified Halbach rings (2)

$$\psi = h_r B_0 - Q_1 B_0 \frac{u_r^2 - h_r^2}{2} - Q_2 B_0 u_r h_r - \frac{u_r^2}{2} \hat{s}' \cdot \mathbf{B}_0$$

$$B_{u_r} = u_r(Q_1 B_0 + \hat{s}' \cdot \mathbf{B}_0) + h_r Q_2 B_0$$

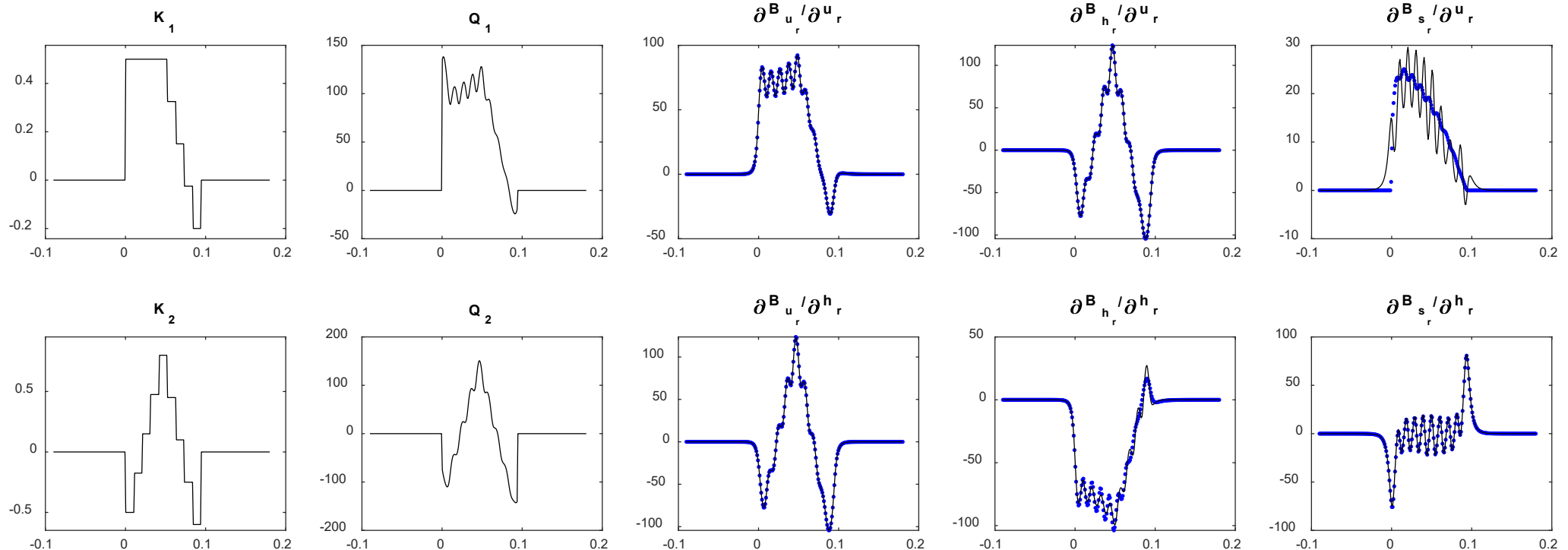
$$B_{h_r} = -B_0 + u_r Q_2 B_0 - h_r Q_1 B_0$$

$$B_s = -h_r B'_0 + u_r \kappa_s B_0$$

Actual quadrupoles $Q \approx 215 \text{ K}$.

- Q is a “smoothed” version of K
- When $K = 0, Q \neq 0$ since Q definition was made for electrical inflector

Numerical verification of:



Cyclotron model – SPC2

Previous optimization: $\min f$ (emittance and spread)
No real model of the cyclotron acceptance

Simple model of solid pole cyclotron

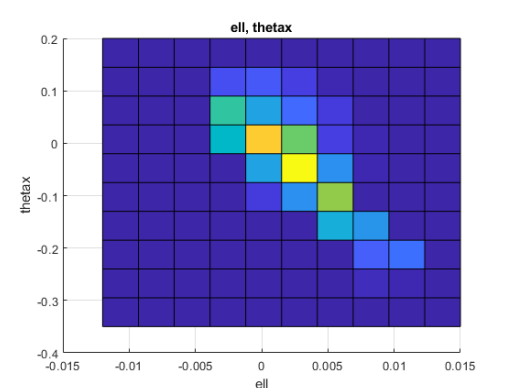
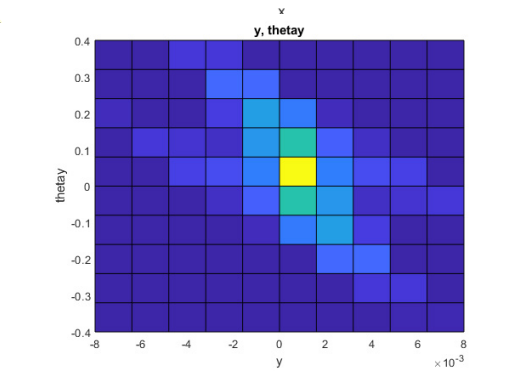
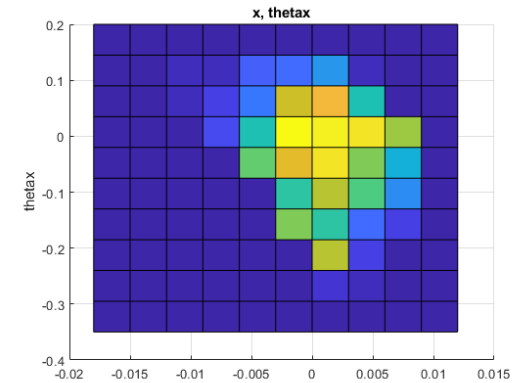
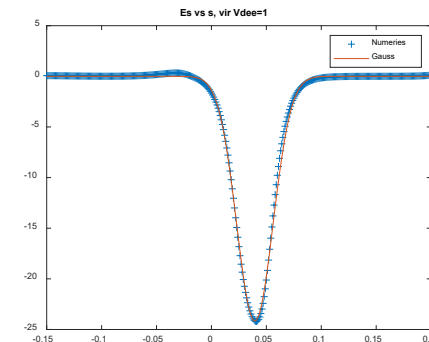
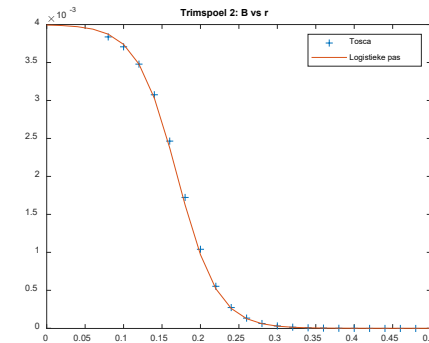
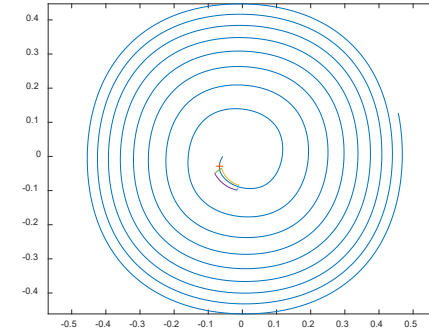
- Main B field is an offset sinusoid
- Flutter disappears in central region
- Trim coils for isochronism (from TOSCA)
- E fields are oscillating DC fields (numerical solutions of Dee-Dummy Dee field)
- Central path obtained by backtracking along the accelerated equilibrium orbit at extraction
- Losses at slits in central region and at large vertical excursions

Injection point: 3 cm in front of first acceleration gap

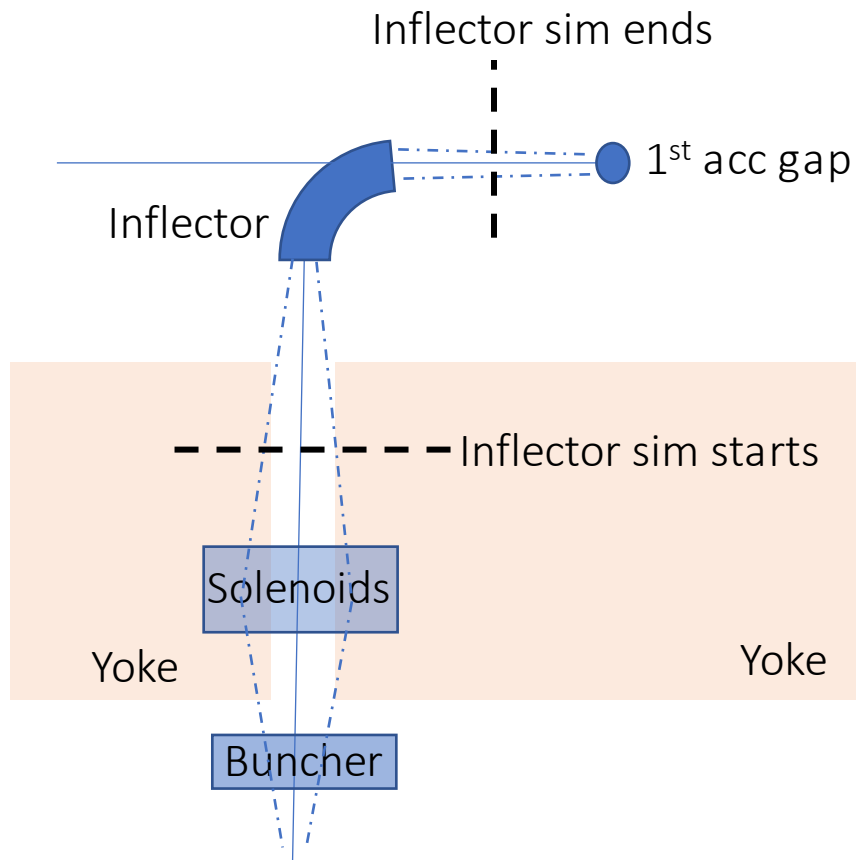
Extraction point: location of electrostatic extraction channel

Acceptance: ellipse

within set distance from sampled points in acceptance



Injection beam line



Inflector simulation:

- starts in region where main magnetic field is zero, based on TOSCA simulation of field in axial hole
- ends in region where inflector field, and acceleration field, are zero

Beam focused at inflector entrance

Buncher

- first harmonic
- focusses at first acceleration gap
- Includes optical length of inflector, R_{56}

Transmission through cyclotron:

1. Pick random particle in DC beam, upstream of buncher
2. Propagate to \mathbf{X}_{in} at inflector start (not linear)
3. $\mathbf{X}_{out} = M\mathbf{X}_{in}$
4. Check if it is in cyclotron acceptance
5. Repeat for $\sim 10^5$ particles

Electrostatic solver (1)

During optimization: need to evaluate lots of inflectors

TOSCA takes too long, needs to change geometry and mesh every time

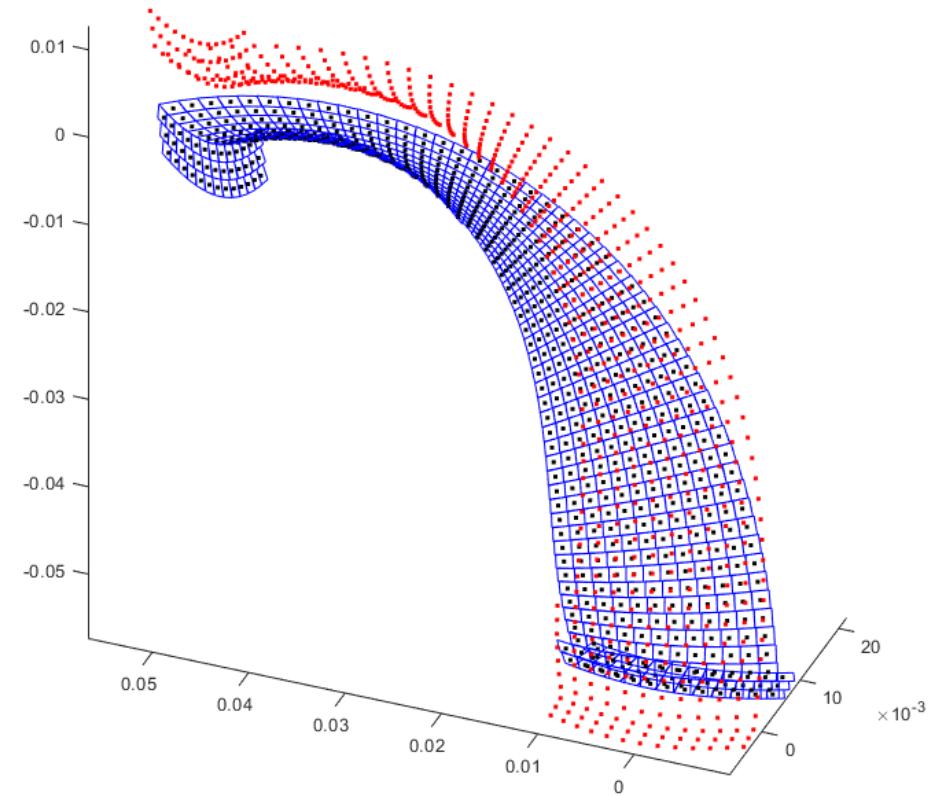
- ~ 1 hour to compute accurate inflector transfer matrix

Previous solution: pre-calculate 7 TOSCA fields and linearly extrapolate

- ~ 5 seconds to compute approximate inflector transfer matrix

New method: compute the surface charge density on the electrodes by minimizing the potential energy

- Only mesh the surface, not the volume
- Compute electric field at any position during run-time
- The field is “smooth”, so integration runs faster
- ~ 3 seconds to compute accurate inflector transfer matrix



Square meshing of negative electrode

Electrostatic solver (2)

Suppose that the surface is divided into approximate squares of side length L_i and charge q_i spread out uniformly over the square

$$U = \frac{1}{2} \mathbf{q} \cdot \mathbf{V}_q + \mathbf{q} \cdot \mathbf{V}_E$$

Write the voltage $\mathbf{V}_q = D\mathbf{q}$

$$D_{ij} = \frac{f_{ij}}{4\pi\epsilon_0|\mathbf{r}_i - \mathbf{r}_j|} \quad f_{ij} \text{ is a geometric factor, set it to 1}$$

Special case $i = j$, self-energy of a square:

$$D_{ii} = \frac{2}{4\pi\epsilon_0q_i^2} \iint \frac{1}{|\mathbf{r}_1 - \mathbf{r}_2|} dq_1 dq_2 = 2 \frac{1.4865}{4\pi\epsilon_0 L_i}$$

Apply a voltage V^n to electrode n by fixing its total charge:

$$\mathbf{q} \cdot \mathbf{c}^n = Q^n$$

where

$$c_i^n = \begin{cases} 1 & \text{if node } i \text{ is part of electrode } n \\ 0 & \text{otherwise} \end{cases}$$

Optimise, using Lagrange multipliers:

$$U = \frac{1}{2} \mathbf{q} \cdot D\mathbf{q} + \mathbf{q} \cdot \mathbf{V}_E + \lambda_1 \mathbf{q} \cdot \mathbf{c}^1 + \dots + \lambda_N \mathbf{q} \cdot \mathbf{c}^N$$

$$D\mathbf{q} + \mathbf{V}_E + (\lambda_1 \mathbf{c}^1 + \dots + \lambda_N \mathbf{c}^N) = 0$$

But $D\mathbf{q} + \mathbf{V}_E$ is the total voltage, so $\lambda_n = -V^n$ and:

$$\lambda_1 \mathbf{c}^1 + \dots + \lambda_N \mathbf{c}^N = -\mathbf{V}$$

In general, solve:

$$\mathbf{q} = D^{-1}(\mathbf{V} - \mathbf{V}_E)$$

$$\mathbf{E}(\mathbf{x}) = \frac{1}{4\pi\epsilon_0} \sum_i q_i \frac{\mathbf{x} - \mathbf{r}_i}{|\mathbf{x} - \mathbf{r}_i|^3}$$

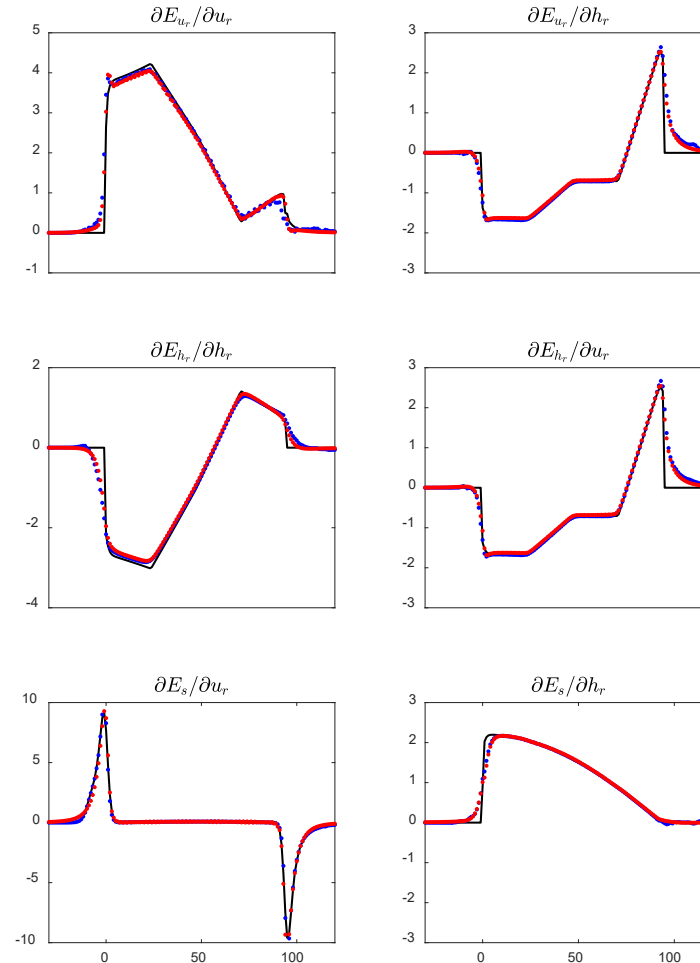
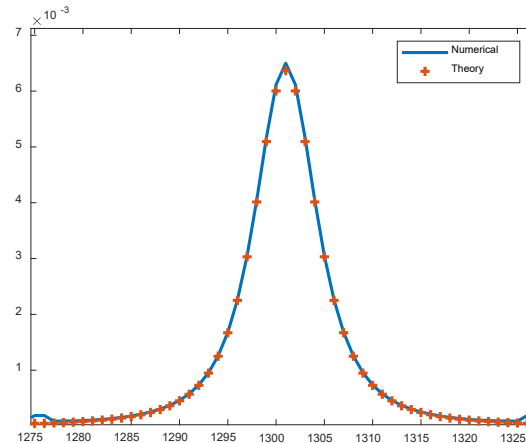
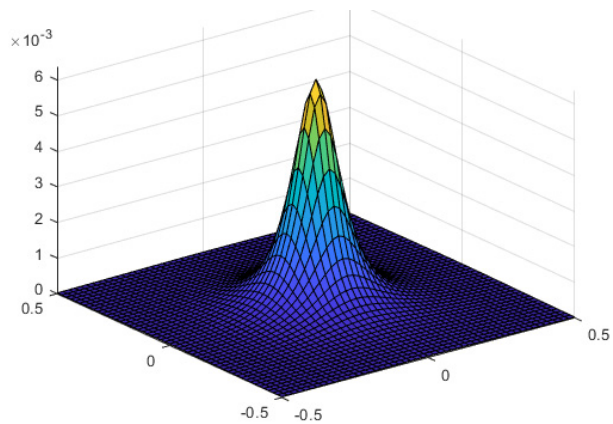
Caveat: \mathbf{x} not close to \mathbf{r}_i

Electrostatic solver (3)

Tests:

- Parallel plate capacitor, E field in middle, error 0.5%
- Surface charge induced in an earthed plate by a point charge
- Inflector: compare to TOSCA and analytic expression

Induced charge



Solid – theory
Blue – TOSCA
Red – this method

Results of optimization

- Optimisation space:
 - Electric: discretize $Q_1(s), Q_2(s)$ into Q_{1i}, Q_{2i} where $i = 1, \dots, 3$
 - Magnetic: K_{1i}, K_{2i} where $i = 1$ to the number of rings
- Cost function: -Transmission through cyclotron
- Method: Random sampling, followed by steepest descent

Transmission Table	Electric Inflector	Magnetic Inflector
Neutral: $Q, K = 0$	26%	33%
Optimised	43%	45%
Relative improvement	65%	36%

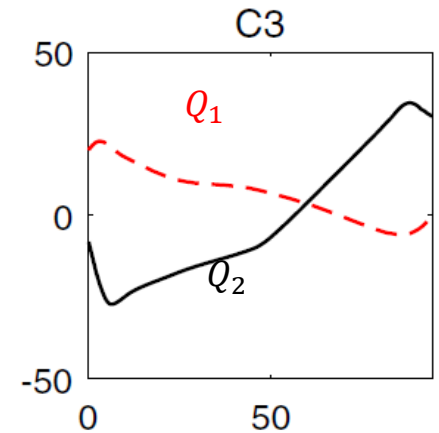
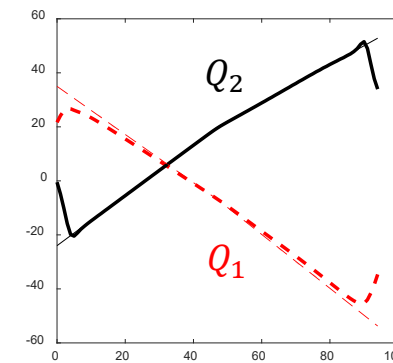
To note:

- Significant improvement
- Similar performance for magnetic and electric
- The electric improvement of 65%, similar to C3 experimental value

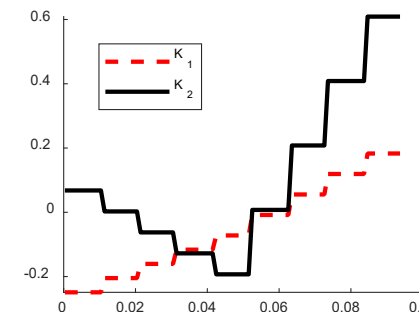
Actual transmission in SPC2 ~5%

- Extraction channel not included in simulation yet, factor ~3 loss
- Emittance of injected beam uncertain

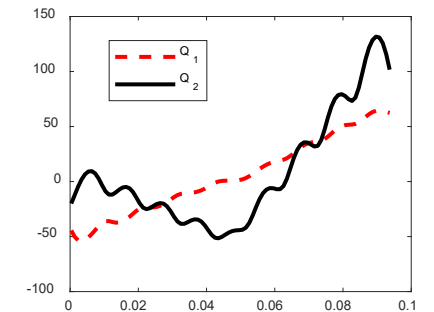
Electric - Similar to C3 design:



Optimal K



Actual Quadrupoles



Conclusion

- Optimisation of inflectors improves performance substantially
- Similar performance from electric and magnetic spiral inflectors

Important:

- Space charge not accounted for (!) so this is strictly speaking only applicable to low intensity machines. But inflector optimization will most probably also be important for high intensity machines.

Thank you!

References

- 1 - Barnard, A. H., et al. "Longitudinal and vertical focusing with a field gradient spiral inflector." *Physical Review Accelerators and Beams* 24.2 (2021): 023501.
- 2 - Ivanenko, I. A. "Methods of compensation of the beam vertical divergence at the exit of spiral inflector in cyclotrons." *Proc. 21st Int. Conf. on Cyclotrons and their Applications (Cyclotrons' 16)*. 2016.
- 3 - Smirnov, V. L. "Central Region Design in a Compact Cyclotron." *Physics of Particles and Nuclei Letters* 16.1 (2019): 34-45.
- 4 - Tsutsui, H. Patent EP2391190A2, JP 2010120716 (2010)
- 5 - Calabretta, Luciano, Mario Maggiore, and Danilo Rifuggiato. "Review of High Power Cyclotrons and Their Applications." *22nd Int. Conf. on Cyclotrons and their Applications (Cyclotrons' 19), Cape Town, South Africa, 23-27 September 2019*. JACOW Publishing, Geneva, Switzerland, 2020.